analytical chemistry

pubs.acs.org/ac Article

Mass-Encoded Suspension Array for Multiplex Detection of Matrix Metalloproteinase Activities

Junjie Hu,[§] Fei Liu,[§] Yunlong Chen, Jia Fu, Guoqiang Shangguan, and Huangxian Ju*

Cite This: *Anal. Chem.* 2022, 94, 6380−6386 Read Online

ACCESS | Metrics & More | Article Recommendations | Supporting Information

ABSTRACT: This work designed a mass spectrometric biosensing strategy for the multiplex detection of matrix metalloproteinases (MMPs) with a mass-encoded suspension array. This array was fabricated as multiplex sensing probes by functionalizing magnetic beads with MMP-specific peptide-isobaric tags for relative and absolute quantification (iTRAQ) conjugates, which contained a hexahistidine tag for surface binding, a substrate region for MMP cleavage, and a coding region for the specific MMP. The integration of the multiplex coding ability of iTRAQ with ultrahigh performance liquid chromatography-tandem mass spectrometry (UPLC-MS/MS) and the proteolysis method for peptide digestion endowed the biosensing method with high throughput and ultrahigh sensitivity. This strategy could be conveniently performed by mixing the sample and the suspension array for enzymatic reactions and then digesting the uncleaved peptides with trypsin to release the coding regions for UPLC-MS/MS analysis. With MMP-2 and MMP-7 as analytes, the relative changes of peak area ratios of coding regions showed good linear responses in the ranges of 0.2−100 and 0.5−400 ng mL^{-1}, with detection limits of 0.064 and 0.17 ng mL^{-1}, respectively. The analysis of MMP activity in serum samples and its change responding to inhibitors demonstrated the specificity, practicability, and expansibility of the proposed strategy. This work paves a new avenue for the activity assays of multiplex enzymes and promotes the development of mass spectrometric biosensing.

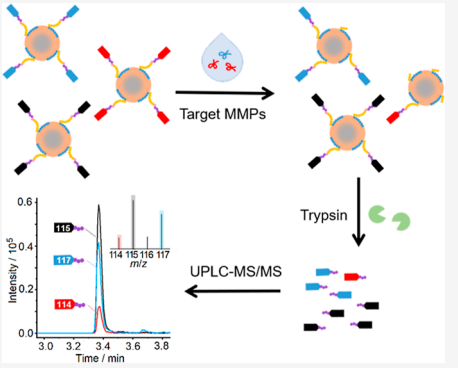

INTRODUCTION

Matrix metalloproteinases (MMPs) are a family of zinc-dependent endopeptidases that are capable of degrading various extracellular matrix proteins.[1−3] More than 26 MMPs have been discovered and proven to play important roles in biological processes such as cell migration, embryogenesis, and tissue remodeling.[4,5] Upregulated expression levels and activities of MMPs are closely associated with pathological progressions of angiogenesis, invasion, and metastasis for cancers. For example, MMP-2 and MMP-9 are overexpressed in breast cancer, cervical cancer, and so forth, while MMP-2 and MMP-7 are reported to correlate with colorectal cancer (CRC).[6,7] Therefore, MMPs can be considered as potential biomarkers for the accurate diagnosis of cancer and the comprehensive assessment of disease progression.

Several approaches have been developed for the sensitive detection of MMPs. The most widely used commercial method is the enzyme-linked immunosorbent assay (ELISA), which requires the utilization of expensive antibody reagents.[8] Because the biological functions of MMPs are mainly dependent on their proteolytic activity, the evaluation of the enzymatic activities of MMPs is more clinically significant.[9−11] Thus, a series of cleavage-based methods with substrate peptide-based probes have been presented for the specific interrogation of enzyme activities using colorimetry,[12,13] fluorescence,[14−17] nanopore,[18] or electrochemical[19−21] and eletrochemiluminescence[22] sensors. These strategies generally focus on the assay of single-MMP activity, and the reported multiplex detections with signal tagging at different wavelengths or potentials suffer from the drawbacks of signal overlapping. Thus, it is necessary to develop novel technology for multiplex MMP activity assays to meet the needs of clinical applications.

Recently, the concept of "Mass Spectrometric Biosensing" has been proposed by our group and is considered to be a powerful tool for multiplex analysis.[23,24] It takes the advantages of mass spectrometry (MS) and biosensing technology and can be applied for the analysis of multiplex targets via molecular recognition and mass-tag probes.[24] Among different mass tags which can transfer the information of analytes to explicit mass spectrometric signals, peptides have been used for enzyme activity assays owing to their sequence designability and properties as natural substrates.[25−27] However, searching for and identifying target-related peptides is difficult due to the

Received: February 22, 2022
Accepted: April 1, 2022
Published: April 12, 2022

https://doi.org/10.1021/acs.analchem.2c00854
Anal. Chem. 2022, 94, 6380−6386

Scheme 1. (A) Schematic Illustration of the Preparation of iTRAQ-Coded Peptide-MB Probes; (B) Schematic for the Detections of MMP-2 and MMP-7 Activities by UPLC-MS/MS with the MRM Mode

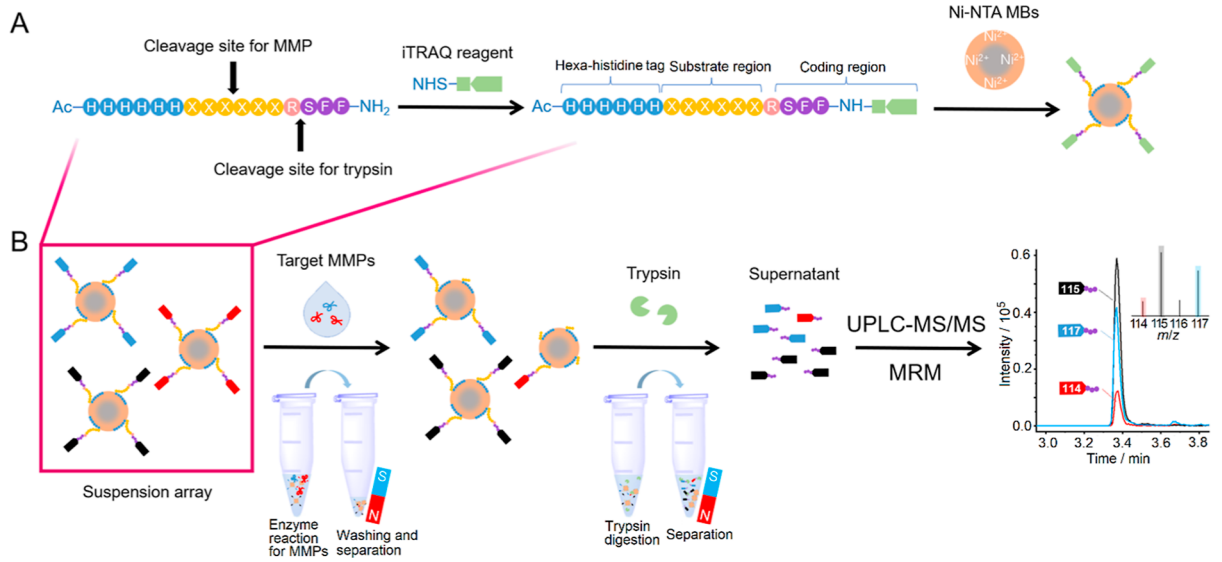

complex interferences in biosamples, and quantitation is another problem because of the ionization differences of multiplex peptide codes.[28] In view of the fact that isobaric tags for relative and absolute quantification (iTRAQ) achieve mass spectrometric quantification in proteomics[29−32] and can avoid mass heterogeneity,[33,34] this work introduced iTRAQ as the encoding elements to design a mass-encoded suspension array for multiplex mass spectrometric biosensing of MMP activity.

The designed mass-encoded suspension array integrated the advantages of MMP enzymatic cleavage for specific peptide sequences, iTRAQ for multiplex coding, magnetic beads (MBs) for rapid separation, and the proteolysis method for peptide digestion and identification with ultrahigh performance liquid chromatography-tandem MS (UPLC-MS/MS). It was fabricated as the multiplex iTRAQ-encoded peptide-MB probes with nickel-nitrilotriacetic acid-modified MBs (Ni-NTA MBs) and peptides, which included a hexahistidine tag for strongly binding to Ni-NTA MBs, the substrate for recognition and cleavage of the target MMP, or service as control, and the sequence -RSFF-NH_2 for covalently conjugation with the iTRAQ (Scheme 1A). The component with specific sequences of SFF-iTRAQ was used for coding the target MMP. The detection workflow involved two proteolysis treatments: first, the respective probes were cleaved by target MMP-2 and MMP-7, followed by magnetic separation and washing steps to remove the sample solution and cleaved peptides; and then trypsin was added to digest the rest of the uncleaved peptides on the MB surfaces at the C-terminal of the Arg residue, to release the specific coding regions of SFF-iTRAQs into the supernatant for UPLC-MS/MS analysis with the multiple reaction monitoring (MRM) mode, in which the peak area at the fixed retention time negatively correlated with the respective target MMP (Scheme 1B). The relative change in the peak area ratio of coding regions showed a good linear response to the MMP activity, leading to a sensitive sensing method for the multiplex detection of MMP activity. The excellent analytical performance of the proposed biosensing strategy for practical samples demonstrated its potential application in biomedicine and clinical diagnosis.

EXPERIMENTAL SECTION

Preparation of iTRAQ-Coded Peptide-MB Probes. The synthesis of peptide-iTRAQ conjugates is described and shown in the Supporting Information (Scheme S1). The peptide-iTRAQ conjugates were bound to the surface of Ni-NTA Dynabeads through the chelation between Ni^{2+} and his-tag peptides. First of all, a 50 μL suspension of Ni-NTA MBs (2 mg MBs) was transferred to a microcentrifuge tube after rotating for 5 min for thorough suspending. The tube was placed on a magnet for 2 min to discard the supernatant. Then, a 100 μL of P1-iTRAQ114, P2-iTRAQ117, or P3-iTRAQ115 solution and 600 μL of binding buffer (50 mM sodium phosphate, pH 8.0, 300 mM NaCl, and 0.01% Tween-20) were added to the MB suspension to incubate for 10 min at room temperature (Scheme S2). After the supernatant was discarded, the MBs were washed with 400 μL of binding buffer three times. The iTRAQ-coded peptide-MB probes (Probe 1, Probe 2, and Probe 3) were suspended in 400 μL of binding buffer and stored at 4 °C for further use.

Detection of MMP-2 and MMP-7 Activities. The prepared Probes 1−3 were mixed with equal amounts to obtain the mass-encoded suspension array. 20 μL of the array was then transferred to a microtube, followed by magnetic separation to discard the supernatant. Subsequently, 20 μL of single MMP-2 or MMP-7, the mixture of MMP-2 and MMP-7 at various concentrations (0, 0.2, 1.0, 5.0, 10, 25, 50, 75, 100, 150, and 200 ng mL^{-1} for MMP-2 and 0, 0.5, 2.0, 20, 50, 150, 250, 400, 500, 750, and 1000 ng mL^{-1} for MMP-7), the mixture of MMPs with the inhibitor BB-94, or 5× diluted serum samples in TCNB buffer (50 mM tris, pH 7.6, 150 mM NaCl, 5 mM $CaCl_2$, and 0.05% Brij) were added to the probes to incubate at 37 °C for 2 h. After placing the tube on a magnet for 2 min, removing the supernatant, and washing with TCNB buffer, 50 μL of 50 ng mL^{-1} trypsin in 25 mM NH_4HCO_3 was added to the microtube for 30 min to digest the uncleaved peptide-iTRAQ conjugates. The supernatant was then diluted to a fivefold volume with acetonitrile containing 1% formic acid and subjected to analysis using UPLC-MS/MS. All the experiments were performed in triplicate.

https://doi.org/10.1021/acs.analchem.2c00854
Anal. Chem. 2022, 94, 6380−6386

UPLC-MS/MS Analysis. The UPLC-MS/MS experiments were carried out on an LC30A UPLC system (Shimadzu, Japan) coupled with a QTRAP 5500 apparatus (AB Sciex, USA). The samples were separated using a Kinetex Biphenyl 100 Å column (100 × 3.0 mm, 2.6 μm, Phenomenex, USA) at a constant flow rate of 0.5 mL min^{-1}. 5 mM NH_4OAc containing 0.1% formic acid was used as mobile phase A, and methanol containing 0.1% formic acid was used as mobile phase B. The elution gradients were as follows: 0.0−1.0 min 5% B, 1.0−1.1 min 5%−20% B, 1.3−3.0 min 20%−95% B, 3.0−4.2 min 95% B, 4.2−4.3 min 95%−5% B, 4.3−5.0 min 5% B, and 5.0 min Stop, and the injection volume was 2 μL. The 5500 QTRAP with an electrospray ionization source was operated in the positive MRM mode, with optimal acquisition parameters as follows: curtain gas (30), ionspray voltage (5500), ion source gas 1 (45), ion source gas 2 (30), source temperature (550 °C), collision gas (high), declustering potential (90), entrance potential (10), and collision cell exit potential (15). The transitions and collision energies (CEs) of the iTRAQ-labeled product peptides (coding regions) were tuned to optimize the fragment intensity (Table 1). The resolution parameters of the first and third quadrupoles were set as the "unit". The target ions were transmitted with a narrow window (0.5 Da). The dwell time was 100 ms for every transition. Data analysis was performed using Analyst and MultiQuant from AB Sciex (USA).

Table 1. Optimization of Transitions and CEs for Peptide Coding Regions

coding region	Q1	Q3	CE
SFF-iTRAQ114	544.5	114.1	35
SFF-iTRAQ117	544.5	117.1	35
SFF-iTRAQ115	544.5	115.1	35

RESULTS AND DISCUSSION

Fabrication of iTRAQ-Coded Peptide-MB Probes. The preparation of P1-iTRAQ114, P2-iTRAQ117, and P3-iTRAQ115 was confirmed by matrix-assisted laser desorption/ionization MS (MALDI-MS), which showed the mass shift of +145 Da and indicated the conjugation process (Figure S1).

To evaluate the binding amount of peptide-iTRAQ on each MB, an elution buffer that contained imidazole was used for the elution of P1-iTRAQ114, P2-iTRAQ117, and P3-iTRAQ115 from Probes 1, 2, and 3, and the absorbance value of the eluted solution at 258 nm or 280 nm was measured to calculate the peptide concentrations according to the absorbance properties of the aromatic amino acids contained in the peptide sequences.[35] From the size of MBs (1 μm), the density of Dynabeads (1.23 g cm^{-3}) and the weight of one MB (6.43×10^{-13} g), 50 μL (2 mg) of the MB solution totally contained 3.11×10^9 beads, and the average number of P1-iTRAQ114, P2-iTRAQ117, and P3-iTRAQ115 binding to each MB was estimated to be 6.95×10^6, 2.51×10^6, and 5.44×10^6, respectively (Figure S2). The difference in binding amounts could be attributed to factors such as the sequence, structure, and net charge of the designed peptides. A large number of peptide-iTRAQs on MBs could improve the detection sensitivity.

Feasibility of the Sensing Strategy. To demonstrate the feasibility of the mass spectrometric sensing strategy, the mixed Probes 1−3 (suspension array) were, respectively, incubated with blank TCNB buffer, single MMP-2 or MMP-7, and their mixture for 2 h, followed by magnetic separation, washing, and trypsinization, and the supernatants were subjected to UPLC-MS/MS analysis. Extracted MRM chromatograms showed the peaks for peptide coding regions of SFF-iTRAQ114, SFF-iTRAQ117, and SFF-iTRAQ115 at a retention time of 3.38 min (Figure 1A−D). Compared with the blank (Figure 1A),

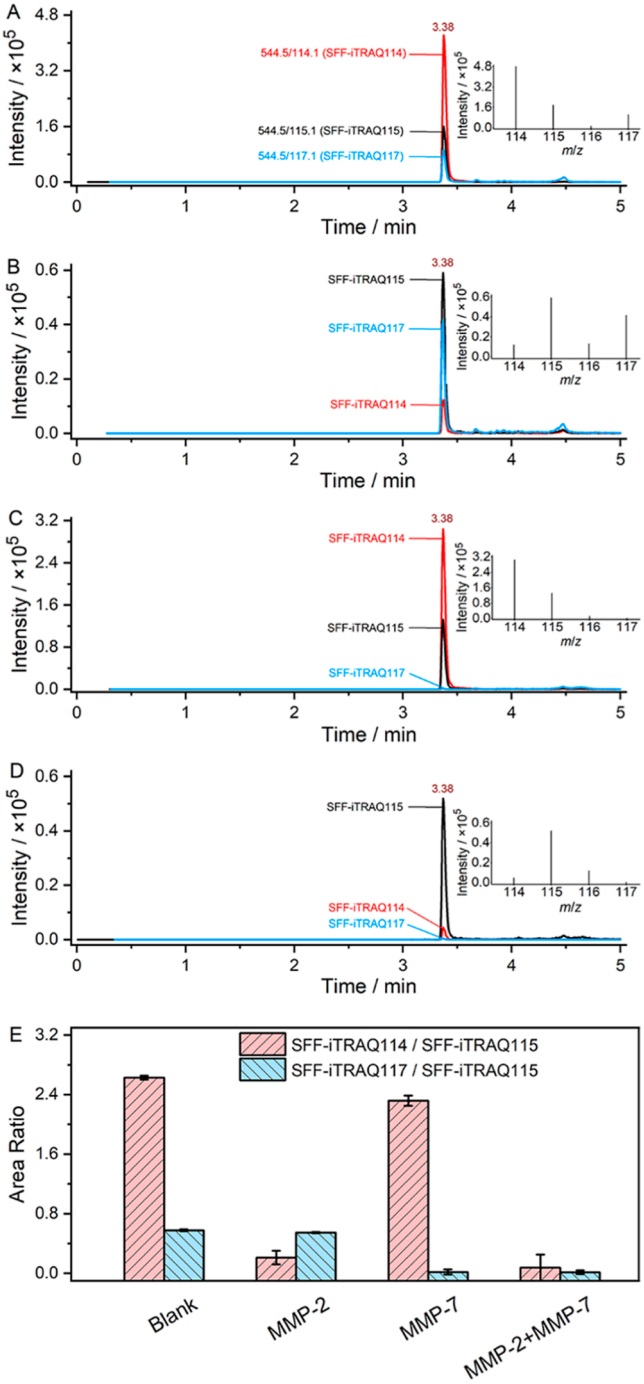

Figure 1. Extracted MRM chromatograms of coding regions of SFF-iTRAQ114, SFF-iTRAQ117, and SFF-iTRAQ115 from the supernatant after treating Probes 1−3 with (A) blank buffer, (B) 200 ng mL^{-1} MMP-2, (C) 1000 ng mL^{-1} MMP-7, and the (D) mixture of 200 ng mL^{-1} MMP-2 and 1000 ng mL^{-1} MMP-7, and then digesting with trypsin. (E) Peak area ratios of SFF-iTRAQ114/SFF-iTRAQ115 and SFF-iTRAQ117/SFF-iTRAQ115 for samples (A−D).

https://doi.org/10.1021/acs.analchem.2c00854
Anal. Chem. 2022, 94, 6380−6386

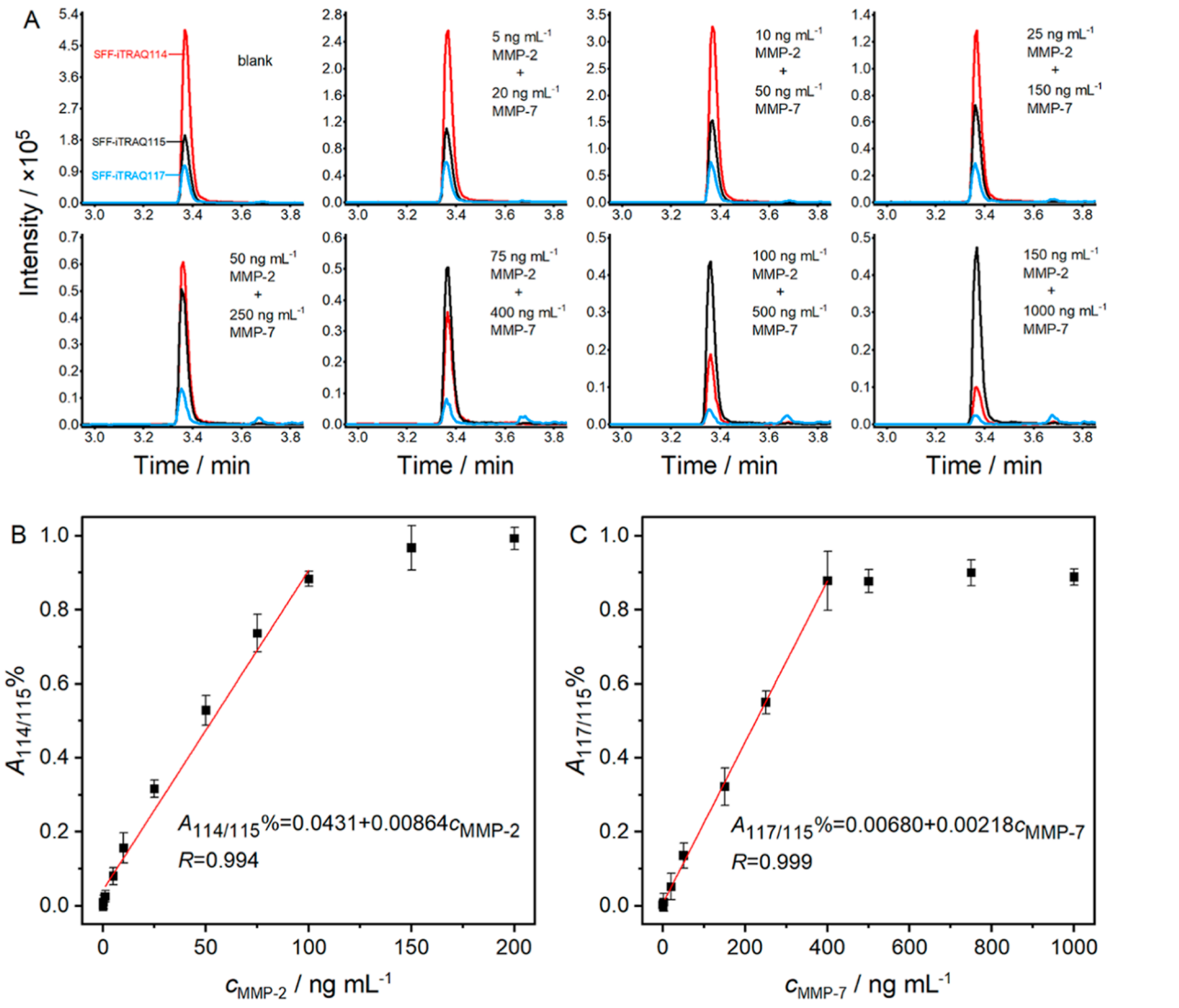

Figure 2. (A) Representative extracted MRM chromatograms of coding regions of SFF-iTRAQ114, SFF-iTRAQ117, and SFF-iTRAQ115 from the supernatants after treating the probes with MMP-2 and MMP-7, and then digesting with trypsin. The plots of the relative changes of peak area ratios (B) $A_{114/115}$ % and (C) $A_{117/115}$ % vs the concentrations of MMP-2 and MMP-7.

the peak intensity for SFF-iTRAQ114 and SFF-iTRAQ117 solely declined in the presence of MMP-2 or MMP-7 (Figure 1B,C), while their intensities dramatically decreased in the presence of MMP-2 and MMP-7 (Figure 1D). Considering that Probe 3 served as control and could not be cleaved by target MMP-2 or MMP-7, the coding region of SFF-iTRAQ115 was completely released by trypsin digestion, and the released amount should theoretically remain constant per test, thus it could be used as an internal standard to correct the matrix interference for quantitation. As shown in Figure 1E, the peak area ratios of SFF-iTRAQ114/SFF-iTRAQ115 and SFF-iTRAQ117/SFF-iTRAQ115 declined with target MMP concentration, indicating Probe 1 and Probe 2 were specific to MMP-2 and MMP-7, respectively, and showed little cross influence between different targets, which was also confirmed by MALDI-MS (Figure S3). The results demonstrated the feasibility of the designed probes for simultaneous detection of MMP-2 and MMP-7 activities.

Quantitative Detections of MMP-2 and MMP-7 Activities. To ensure complete digestion of uncleaved peptide-iTRAQ conjugates to release the coding regions, the experimental concentration for the tool enzyme trypsin was optimized by incubating Probes 1−3 with trypsin at various concentrations (0−100 ng mL^{-1}) and analyzing the respective supernatant by UPLC-MS/MS. The sum of peak areas for SFF-iTRAQ114, SFF-iTRAQ117, and SFF-iTRAQ115 trended to the maximum when the trypsin concentration was 50 ng mL^{-1}, indicating complete release of the coding regions (Figure S4). The cleavage dynamics of MMP-2 and MMP-7 were also examined by incubating Probes 1−3 with targets for different durations. Both the peak area ratios of SFF-iTRAQ114/SFF-iTRAQ115 and SFF-iTRAQ117/SFF-iTRAQ115 decreased with the increasing incubation time until reaching a plateau at 2 h, suggesting the completion of enzyme reactions (Figure S5). Thus, the incubation time of 2 h for MMPs and 50 ng mL^{-1} trypsin for digestion were selected for the following experiments.

Under the optimized conditions, MMP-2 and MMP-7 at various concentrations were mixed with the probes for activity assays following the process described above. The extracted MRM chromatograms showed the decreasing peak area ratios of SFF-iTRAQ114/SFF-iTRAQ115 and SFF-iTRAQ117/SFF-

https://doi.org/10.1021/acs.analchem.2c00854
Anal. Chem. 2022, 94, 6380−6386

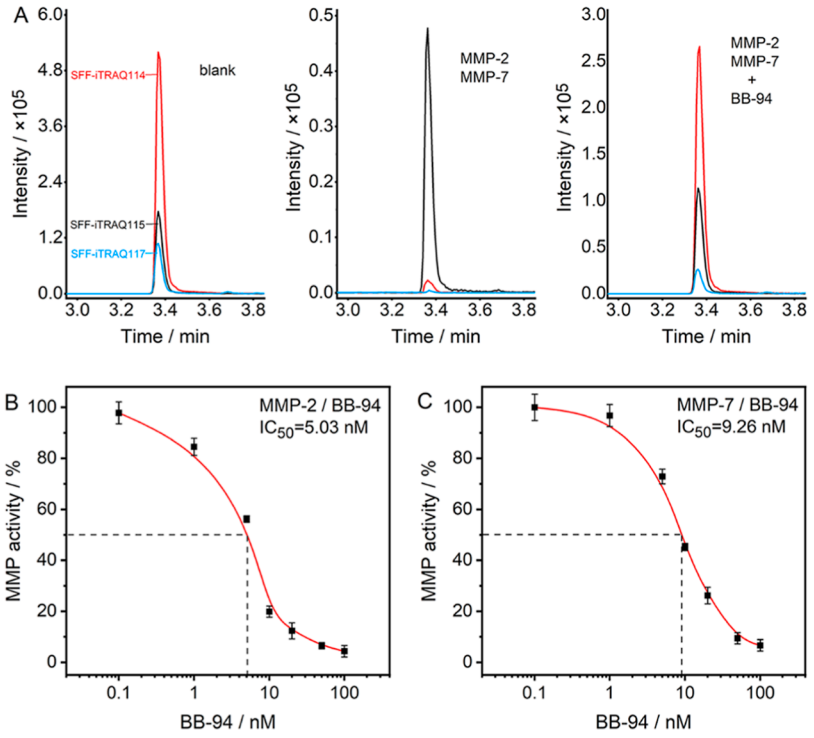

Figure 3. (A) Extracted MRM chromatograms of the supernatants after treating Probes 1−3 with blank TCNB buffer, and the mixture of 200 ng mL^{-1} MMP-2 and 1000 ng mL^{-1} MMP-7 in the absence and presence of 100 nM inhibitor BB-94 and then digesting with trypsin. Plots of enzyme activity for (B) 200 ng mL^{-1} MMP-2 and (C) 1000 ng mL^{-1} MMP-7 vs the logarithm of BB-94 concentration.

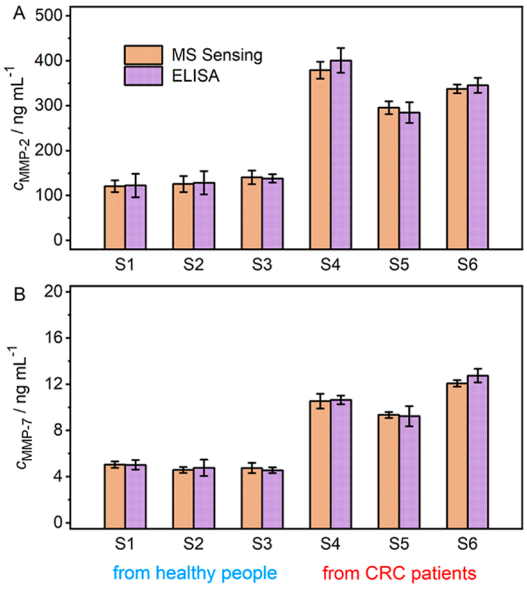

Figure 4. (A) MMP-2 and (B) MMP-7 levels in serum samples analyzed with the proposed mass spectrometric biosensing strategy and ELISA kits.

iTRAQ115 with the increasing concentrations of MMP-2 and MMP-7, respectively (Figures 2A and S6). The plots of the relative changes of peak area ratios ($A_{114/115}$ % and $A_{117/115}$ %) versus the concentrations of MMP-2 and MMP-7 showed good linearity in the ranges of 0.2−100 and 0.5−400 ng mL^{-1}, respectively (Figure 2B,C). Here, $A_{114/115}$ % = 1 − $(A_{\text{SFF-iTRAQ114}}/A_{\text{SFF-iTRAQ115}})/(A_{0,\text{SFF-iTRAQ114}}/A_{0,\text{SFF-iTRAQ115}})$, while $A_{117/115}$ % = 1 − $(A_{\text{SFF-iTRAQ117}}/A_{\text{SFF-iTRAQ115}})/(A_{0,\text{SFF-iTRAQ117}}/A_{0,\text{SFF-iTRAQ115}})$, in which $A_{\text{SFF-iTRAQ114}}$, $A_{\text{SFF-iTRAQ117}}$, and $A_{\text{SFF-iTRAQ115}}$ and $A_{0,\text{SFF-iTRAQ114}}$, $A_{0,\text{SFF-iTRAQ117}}$, and $A_{0,\text{SFF-iTRAQ115}}$ represent the peak areas in the presence and in the absence of the related target MMP, respectively. The detection limits for MMP-2 and MMP-7 were calculated to be 0.064 and 0.17 ng mL^{-1} at 3σ, respectively. The proposed mass spectrometric biosensing strategy showed satisfactory analytical performance that is comparable with the previously reported literature (Table S1).

Analysis of the MMP Inhibitor. The mass spectrometric biosensing method was verified with the inhibition effect of batimastat, which is known as BB-94 and acts as a potent MMP inhibitor.[36] In the presence of BB-94 in the MMP solution, the peak intensities for both SFF-iTRAQ114 and SFF-iTRAQ117, and the peak area ratios for SFF-iTRAQ114/SFF-iTRAQ115 and SFF-iTRAQ117/SFF-iTRAQ115 dramatically increased compared to those without the presence of BB-94 (Figure 3A), suggesting the decreased cleavage of Probe 1 and Probe 2. Thus, BB-94 inhibited the activities of both MMP-2 and MMP-7. The IC50 (defined as 50% inhibition efficiency) of BB-94 toward MMP-2 and MMP-7 was estimated to be 5.03 and 9.26 nM, respectively (Figure 3B,C), which was close to previously reported 4 and 6 nM, respectively.[37] The results demonstrated the application of the mass spectrometric biosensing strategy in screening and assessing MMP inhibitors.

Specificity and Reproducibility. The specificity of the proposed method was investigated by comparing the relative changes of peak area ratios of SFF-iTRAQ114/SFF-iTRAQ115 and SFF-iTRAQ117/SFF-iTRAQ115 toward respective targets MMP-2 and MMP-7, and other enzymes (or protein) such as MMP-1, MMP-3, caspase-3, caspase-8, and bovine serum albumin. The relative changes of peak area ratios caused by MMP-2 and MMP-7 were 6−50 times higher

https://doi.org/10.1021/acs.analchem.2c00854
Anal. Chem. 2022, 94, 6380−6386

than those by other MMPs and proteases (Figure S7), indicating good specificity of the proposed strategy.

The reproducibility of the proposed strategy was examined with interassay tests by measuring 1.0, 10, and 50 ng mL^{-1} MMP-2 and 2.0, 50, and 250 ng mL^{-1} MMP-7 with six suspension arrays fabricated under the same experimental condition. The relative changes of related area ratios showed the RSDs of 5.6, 4.2, and 3.3% for MMP-2, and 4.4, 4.1, and 5.2% for MMP-7, respectively, suggesting acceptable precision and reproducibility of the mass spectrometric biosensing strategy.

Determinations of MMPs in Clinical Samples. The proposed strategy was used for the determination of MMP-2 and MMP-7 in clinical samples. Serum samples from three healthy people and three CRC patients were analyzed. Considering the normal MMP levels in human serum samples and the linear ranges of the proposed method, the samples were diluted fivefold before the test. The test results were highly consistent with those obtained by the commercial ELISA kits, with relative errors in the range of −9.46−4.18% (Table S2). It should be noted that the ELISA method can detect the total MMP levels (proMMPs and active MMPs) via immunological recognition, while the MS-based method measures only the active form of MMPs.[6] Generally, proMMP-2 and proMMP-7 are captured on cell membranes, which means that most secreted MMP-2 and MMP-7 in serum are activated, accounting for the consistent results obtained with the two methods,[1,38] and thus the two methods can verify each other.[39] The average levels of MMP-2 and MMP-7 in serum samples from the three CRC patients were 337.2 and 10.65 ng mL^{-1}, respectively, which were more than twofold higher than those (128.9 ng mL^{-1} for MMP-2 and 4.79 ng mL^{-1} for MMP-7) from healthy people (Table S2 and Figure 4). This resulted from the overexpression of MMP-2 and MMP-7 in the processes of CRC tumor cell growth and metastasis.[40] To demonstrate the practical applications, the levels of MMP-2 and MMP-7 in a batch of serum samples from 20 CRC patients and 12 healthy people, whose clinical information is listed in Table S3, were further tested with the MS-based method to picture the two-dimensional (2D) scatter diagram, which showed an obvious aggregation tendency within the respective CRC patients and healthy people (Figure S8). Thus, the proposed strategy is suitable for practical applications and possesses great potential for early diagnosis and progression assessment of cancer.

CONCLUSIONS

This work develops a mass spectrometric biosensing strategy for the multiplex detection of MMP activities with a designed mass-encoded suspension array. The suspension array contains multiplex iTRAQ-coded peptide-MB probes, which are prepared by functionalizing Ni-NTA MBs with peptide-iTRAQ conjugates. The conjugates contain a his-tag for binding to the bead surface, the substrate region for cleavage of the corresponding MMP, and the coding region. The strategy can be simply performed by mixing the suspension array with samples for enzyme reactions, followed by digesting the uncleaved probes with trypsin to release the coding regions for UPLC-MS/MS analysis. The relative changes in area ratios of coding regions show good linearity with the activity or concentration of target MMPs. The proposed iTRAQ-coded biosensing approach exhibits high specificity toward targets MMP-2 and MMP-7 and has been used for inhibition analysis and MMP activity assays in serum samples from healthy people and CRC patients, showing great potential in the screening of anticancer agents and early diagnosis of cancer. This strategy combines the advantages of proteomics and mass spectrometric biosensing and paves a new avenue for multiplex enzyme analysis. It can be further expanded by designing different enzyme-specific peptide substrates along with 8-plex iTRAQ or even 10-plex Tandem Mass Tag (TMT) reagents as coding elements for simultaneous and accurate multiplex enzyme assays in various biosamples.

ASSOCIATED CONTENT

Supporting Information

The Supporting Information is available free of charge at https://pubs.acs.org/doi/10.1021/acs.analchem.2c00854.

Materials and reagents, additional experimental details, scheme for preparation of peptide-iTRAQ conjugates; MALDI-TOF mass spectra of the peptides, peptide-iTRAQ conjugates and their responses to target MMPs; number of the conjugates immobilized on each bead, optimization of trypsin concentrations and incubation time; results of UPLC-MS/MS analysis, specificity of the method, 2D scatter profile of MMPs for serum samples, comparison of assay performances, detection results of MMPs in human serum samples, and clinical information of serum samples (PDF)

AUTHOR INFORMATION

Corresponding Author

Huangxian Ju − *State Key Laboratory of Analytical Chemistry for Life Science, School of Chemistry and Chemical Engineering, Nanjing University, Nanjing 210023, China;* orcid.org/0000-0002-6741-5302; Phone: +86-25-89683593; Email: hxju@nju.edu.cn

Authors

Junjie Hu − *College of Forensic Medicine and Laboratory Medicine, Jining Medical University, Jining 272067, China; State Key Laboratory of Analytical Chemistry for Life Science, School of Chemistry and Chemical Engineering, Nanjing University, Nanjing 210023, China*

Fei Liu − *State Key Laboratory of Analytical Chemistry for Life Science, School of Chemistry and Chemical Engineering, Nanjing University, Nanjing 210023, China*

Yunlong Chen − *State Key Laboratory of Analytical Chemistry for Life Science, School of Chemistry and Chemical Engineering, Nanjing University, Nanjing 210023, China;* orcid.org/0000-0002-3775-3028

Jia Fu − *College of Forensic Medicine and Laboratory Medicine, Jining Medical University, Jining 272067, China*

Guoqiang Shangguan − *College of Forensic Medicine and Laboratory Medicine, Jining Medical University, Jining 272067, China*

Complete contact information is available at: https://pubs.acs.org/10.1021/acs.analchem.2c00854

Author Contributions

[§]J.H. and F.L. contributed equally to this work.

Notes

The authors declare no competing financial interest.

https://doi.org/10.1021/acs.analchem.2c00854
Anal. Chem. 2022, 94, 6380−6386

■ ACKNOWLEDGMENTS

This work was financially supported by the National Natural Science Foundation of China (21904049, 21827812, and 21974063), the Natural Science Foundation of Shandong Province (ZR2019BB037), and the Faculty Start-up Funds of Jining Medical University (2017JYQD04). We specially thank Na Xie and Dr. Bin Zhang in the Department of Laboratory Medicine, Affiliated Hospital of Jining Medical University, for providing serum samples from healthy people and CRC patients.

■ REFERENCES

(1) Egeblad, M.; Werb, Z. *Nat. Rev.* **2002**, *2*, 161−174.
(2) Visse, R.; Nagase, H. *Circ. Res.* **2003**, *92*, 827−839.
(3) Shapiro, S. D. *Curr. Opin. Cell Biol.* **1998**, *10*, 602−608.
(4) Gong, T.; Kong, K. V.; Goh, D.; Olivo, M.; Yong, K.-T. *Biomed. Opt. Express* **2015**, *6*, 2076−2087.
(5) Jonsson, A.; Hjalmarsson, C.; Falk, P.; Ivarsson, M.-L. *Br. J. Cancer* **2016**, *115*, 703−706.
(6) Lei, Z.; Jian, M.; Li, X.; Wei, J.; Meng, X.; Wang, Z. *J. Mater. Chem. B* **2020**, *8*, 3261−3291.
(7) Li, H.; Qiu, Z.; Li, F.; Wang, C. *Oncol. Lett.* **2017**, *14*, 5865−5870.
(8) Yu, J.; He, Z.; He, X.; Luo, Z.; Lian, L.; Wu, B.; Lan, P.; Chen, H. *Front. Oncol.* **2021**, *11*, 771099.
(9) Patel, S.; Sumitra, G.; Koner, B. C.; Saxena, A. *Clin. Biochem.* **2011**, *44*, 869−872.
(10) Hu, Q.; Su, L.; Mao, Y.; Gan, S.; Bao, Y.; Qin, D.; Wang, W.; Zhang, Y.; Niu, L. *Biosens. Bioelectron.* **2021**, *178*, 113010.
(11) Yin, L.; Sun, H.; Zhang, H.; He, L.; Qiu, L.; Lin, J.; Xia, H.; Zhang, Y.; Ji, S.; Shi, H.; Gao, M. *J. Am. Chem. Soc.* **2019**, *141*, 3265−3273.
(12) Cheng, W.; Chen, Y.; Yan, F.; Ding, L.; Ding, S.; Ju, H.; Yin, Y. *Chem. Commun.* **2011**, *47*, 2877−2879.
(13) Kim, G. B.; Kim, K. H.; Park, Y. H.; Ko, S.; Kim, Y.-P. *Biosens. Bioelectron.* **2013**, *41*, 833−839.
(14) Jian, M.; Su, M.; Gao, J.; Wang, Z. *Sens. Actuators, B* **2020**, *304*, 127320.
(15) Zeng, W.; Wu, L.; Sun, Y.; Wang, Y.; Wang, J.; Ye, D. *Small* **2021**, *17*, 2101924.
(16) Cao, S.; Li, Z.; Zhao, J.; Chen, M.; Ma, N. *ACS Sens.* **2018**, *3*, 1522−1530.
(17) Zhang, Y.; Chen, X.; Yuan, S.; Wang, L.; Guan, X. *Anal. Chem.* **2020**, *92*, 15042−15049.
(18) Wang, H.; Huang, W.; Wang, Y.; Li, W.; Liu, Q.; Yin, B.; Liang, L.; Wang, D.; Guan, X.; Wang, L. *ACS Sens.* **2021**, *6*, 3781−3788.
(19) Palomar, Q.; Xu, X.; Selegård, R.; Aili, D.; Zhang, Z. *Sens. Actuators, B* **2020**, *325*, 128789.
(20) Xi, X.; Wen, M.; Song, S.; Zhu, J.; Wen, W.; Zhang, X.; Wang, S. *Chem. Commun.* **2020**, *56*, 6039−6042.
(21) Chen, Y.; Song, X.; Li, L.; Tang, B. *Anal. Chem.* **2020**, *92*, 5855−5861.
(22) Gao, H.; Dang, Q.; Xia, S.; Zhao, Y.; Qi, H.; Gao, Q.; Zhang, C. *Sens. Actuators, B* **2017**, *253*, 69−76.
(23) Feng, N.; Hu, J.; Ma, Q.; Ju, H. *Biosens. Bioelectron.* **2020**, *157*, 112159.
(24) Hu, J.; Liu, F.; Chen, Y.; Shangguan, G.; Ju, H. *ACS Sens.* **2021**, *6*, 3517−3535.
(25) Hu, J.; Liu, F.; Ju, H. *Anal. Chem.* **2015**, *87*, 4409−4414.
(26) Hu, J.; Liu, F.; Ju, H. *Angew. Chem., Int. Ed.* **2016**, *55*, 6667−6670.
(27) Hu, J.; Liu, F.; Feng, N.; Ju, H. *Rapid Commun. Mass Spectrom.* **2016**, *30*, 196−201.
(28) Hu, J.; Liu, F.; Feng, N.; Ju, H. *Anal. Chim. Acta* **2019**, *1064*, 1−10.
(29) Ludwig, K. R.; Dahl, R.; Hummon, A. B. *J. Proteome Res.* **2016**, *15*, 1497−1505.
(30) Pichler, P.; Köcher, T.; Holzmann, J.; Mazanek, M.; Taus, T.; Ammerer, G.; Mechtler, K. *Anal. Chem.* **2010**, *82*, 6549−6558.
(31) Chen, C.-J.; Chou, C.-Y.; Shu, K.-H.; Chen, H.-C.; Wang, M.-C.; Chang, C.-C.; Hsu, B.-G.; Wu, M.-S.; Yang, Y.-L.; Liao, W.-L.; Yang, C.; Hsiao, Y.-T.; Huang, C.-C. *J. Proteome Res.* **2021**, *20*, 2953−2963.
(32) Yu, D.; Wang, Z.; Cupp-Sutton, K. A.; Guo, Y.; Kou, Q.; Smith, K.; Liu, X.; Wu, S. *J. Am. Soc. Mass Spectrom.* **2021**, *32*, 1336−1344.
(33) Wiktorowicz, J. E.; English, R. D.; Wu, Z.; Kurosky, A. *J. Proteome Res.* **2012**, *11*, 1512−1520.
(34) Jylhä, A.; Nättinen, J.; Aapola, U.; Mikhailova, A.; Nykter, M.; Zhou, L.; Beuerman, R.; Uusitalo, H. *Clin. Proteomics* **2018**, *15*, 24.
(35) Schmid, F.-X. Biological Macromolecules: UV-Visible Spectrophotometry. *Encyclopedia of Life Sciences*; Macmillan Publishers Ltd., Nature Publishing Group, 2001.
(36) Botos, I.; Scapozza, L.; Zhang, D.; Liotta, L. A.; Meyer, E. F. *Proc. Natl. Acad. Sci. U.S.A.* **1996**, *93*, 2749−2754.
(37) Laronha, H.; Carpinteiro, I.; Portugal, J.; Azul, A.; Polido, M.; Petrova, K. T.; Salema-Oom, M.; Caldeira, J. *Biomolecules* **2020**, *10*, 717.
(38) Shiomi, T.; Inoki, I.; Kataoka, F.; Ohtsuka, T.; Hashimoto, G.; Nemori, R.; Okada, Y. *Lab. Invest.* **2005**, *85*, 1489−1506.
(39) Wang, Z.; Li, X.; Feng, D.; Li, L.; Shi, W.; Ma, H. *Anal. Chem.* **2014**, *86*, 7719−7725.
(40) Said, A.; Raufman, J.-P.; Xie, G. *Cancers* **2014**, *6*, 366−375.

https://doi.org/10.1021/acs.analchem.2c00854
Anal. Chem. 2022, 94, 6380−6386